JACS
JOURNAL OF THE AMERICAN CHEMICAL SOCIETY
Article
pubs.acs.org/JACS

Exploiting High Pressures to Generate Porosity, Polymorphism, And Lattice Expansion in the Nonporous Molecular Framework $Zn(CN)_2$

Saul H. Lapidus,[†,‡,§] Gregory J. Halder,[†,§] Peter J. Chupas,[†] and Karena W. Chapman*[,†]

[†]X-ray Science Division, Advanced Photon Source and [‡]Materials Science Division, Argonne National Laboratory, Argonne, Illinois, 60439, United States United States

Supporting Information

ABSTRACT: Systematic exploration of the molecular framework material $Zn(CN)_2$ at high pressure has revealed several distinct series of transitions leading to five new phases: four crystalline and one amorphous. The structures of the new crystalline phases have been resolved through *ab initio* structural determination, combining charge flipping and direct space methods, based on synchrotron powder diffraction data. The specific transition activated under pressure depends principally on the pressure-transmitting fluid used. Without fluid or in large molecule fluids (e.g., isopropanol, ethanol, or fluorinert), the high-pressure behavior intrinsic to $Zn(CN)_2$ is observed; the doubly interpenetrated diamondoid framework structure transforms to a distorted, orthorhombic polymorph, $Zn(CN)_2$-II (*Pbca*) at ∼1.50−1.58 GPa with asymmetric displacement of the bridging CN ligand and reorientation of the $Zn(C/N)_4$ tetrahedra. In small molecule fluids (e.g., water, methanol, methanol−ethanol−water), the nonporous interpenetrated $Zn(CN)_2$ framework can undergo reconstructive transitions to porous, non-interpenetrated polymorphs with different topologies: diamondoid (*dia*-$Zn(CN)_2$, $Fd\bar{3}m$, P_{trans} ∼ 1.2 GPa), londaleite (*lon*-$Zn(CN)_2$, $P6_3/mmc$, P_{trans} ∼ 0.9 GPa), and pyrite-like (*pyr*-$Zn(CN)_2$, $Pa\bar{3}$, P_{trans} ∼ 1.8 GPa). Remarkably, these pressure-induced transitions are associated with near 2-fold volume expansions. While an increase in volume with pressure is counterintuitive, the resulting new phases contain large fluid-filled pores, such that the combined solid + fluid volume is reduced and the inefficiencies in space filling by the interpenetrated parent phase are eliminated. That both *dia*-$Zn(CN)_2$ and *lon*-$Zn(CN)_2$ phases were retained upon release to ambient pressure demonstrates the potential for application of hydrostatic pressures to interpenetrated framework systems as a novel means to generate new porous materials.

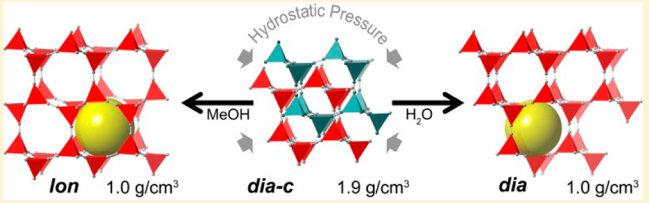

INTRODUCTION

Porosity in open framework materials, such as metal−organic frameworks or MOFs, is highly sought after for applications in guest storage, separation, and sequestration.[1−3] In these materials, not only can the framework components be tuned to access a broad range of pore structures, for a given composition, but also different topologies or polymorphs can often be realized by varying the synthetic conditions.[4,5] In this endeavor, it is generally accepted that to maximize the porosity in a given system, it is important to minimize both the interpenetration of independent frameworks and mechanical stress, which can collapse the pores.[6−8] Indeed, supercritical activation, which minimizes stress when evacuating the pores, has been key to realizing experimental surface areas that approach projected values.[8,9]

Here we demonstrate that mechanical pressure can be exploited to provide a novel and unexpected means to transform a dense interpenetrated framework system into a new porous material. By applying pressures of 0.9−1.8 GPa (∼9000−18 000 atm) to doubly interpenetrated nonporous zinc cyanide, $Zn(CN)_2$,[10] a variety of different structural transitions can be induced. These transitions, and the phases produced, depend on the fluid medium used to transmit pressure to the solid sample. In this way, three new porous phases of different topologies were generated through reconstructive transitions: non-interpenetrated diamondoid (*dia*), lonsdaleite (*lon*), and pyrite (*pyr*). Both the non-interpenetrated diamondoid and lonsdaleite phases could be recovered as metastable phases at ambient pressure. Further nonporous phases were generated through displacive transitions to crystalline and amorphous phases involving static distortions of the original framework structure. We propose that inefficiencies of space-filling in the originally interpenetrated material is key to enabling the counterintuitive decrease in framework density (a volume expansion) under pressure—dense packing of guest molecules from the fluid medium in the newly formed pores contributes to the compression of the combined (solid + fluid) system.

Although the zinc cyanide structure is simple compared to most reported framework materials, as the prototypical molecular framework system, it has had an important role in the development of MOF chemistry in delineating the structure design principles that are now central to the field.[11] Zinc cyanide, $Zn(CN)_2$, consists of tetrahedrally coordinated zinc ions bridged linearly by disordered cyanide anions to form a

Received: February 5, 2013
Published: May 1, 2013

   dx.doi.org/10.1021/ja4012707 | J. Am. Chem. Soc. 2013, 135, 7621−7628

diamondoid or β-cristobalite framework ("*dia*" topology, Figure 1).[10−12] Two independent diamondoid frameworks interpenetrate in the overall cubic system (*Pn*-3*m*, a = 5.9 Å, "*dia-c*" topology). This phase is impermeable to guests at ambient pressure.

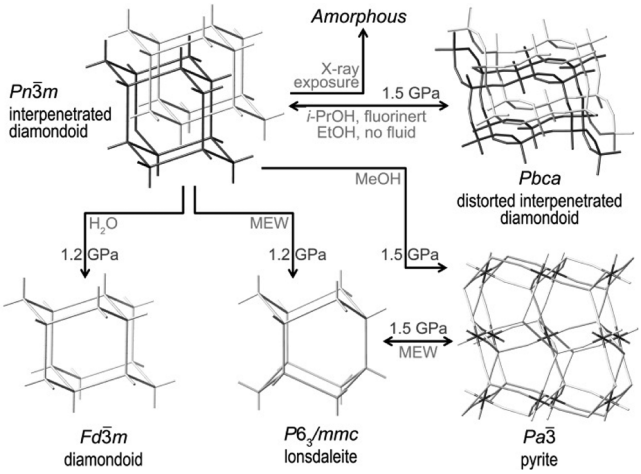

Figure 1. Summary of the various phases formed upon compression of $Zn(CN)_2$ in different fluid media. Phases are shown at the same scale.

While its nonporous structure precludes an exploration of host−guest chemistry, the doubly interpenetrated $Zn(CN)_2$ framework structure is sufficiently open to support pronounced negative thermal expansion (NTE) behavior—an unusual phenomenon with attractive potential applications.[13−15] Transverse vibrations of the cyanide bridge, populated with increasing temperature, induce a contraction of the Zn···Zn′ distance, framework structure, and lattice volume.

The strong potential for pronounced flexibility of the $Zn(CN)_2$ lattice, associated with the low energy characteristic of the lattice modes that contribute to NTE, has motivated high pressure measurements of this system. Measurements below 0.6 GPa, have shown that $Zn(CN)_2$ is highly compressible, with framework softening at higher pressures and an enhancement of the NTE.[15] Several measurements at higher pressures are contradictory.[16,17] These studies do not resolve the high-pressure structure of $Zn(CN)_2$.

EXPERIMENTAL METHODS

Synthesis. Zinc cyanide is highly insoluble. It was prepared by slow diffusion of aqueous solutions of Zn^{2+} and $[Zn(CN)_4]^{2-}$.

High-Pressure Powder Diffraction Measurements. Variable pressure diffraction data were collected in several series of experiments at 1-BM ($\lambda \sim 0.605$ Å), 11-ID-B ($\lambda \sim 0.2128$ Å), and 17-BM (λ = 0.729 Å) at the Advanced Photon Source, at Argonne National Laboratory. Diffraction images were collected with a MAR345 imaging plate area detector or an amorphous silicon-based area detector from Perkin-Elmer (XRD 1621). The raw images were reduced to one-dimensional diffraction data within Fit-2D.[18] Data suitable for structure determination and Rietveld refinement were collected with 30 s exposures. Screw- and membrane-driven diamond anvil cells from Easylab, equipped with ∼500 μm culets, were used to apply pressure to the sample. The sample pressure was estimated based on the compression of an internal diffraction standard with known compressibility, e.g., CaF_2 or NaCl.[19] The sample was loaded in the gasket hole with a small quantity of CaF_2 or NaCl and fluid pressure transmitting media. The high-pressure phase behaviors, and the factors that influence these, were isolated by systematically varying experimental parameters, such as pressure transmitting fluids, compression rates, X-ray exposure, and sample packing. Typical measurements collected data at 0.1−0.2 GPa pressure intervals, with other studies at finer (0.02−0.04 GPa) and coarser (∼0.5 GPa) pressure intervals or with no X-ray exposure below the transition pressure. Pressure transmitting media used include Fluorinert (FC-75), isopropanol, ethanol, methanol, methanol−ethanol−water (16:3:1, MEW), and isopropanol−water (4:1 or 1:1). All alcohols used as pressure-transmitting media were obtained from Sigma-Aldrich as anhydrous fluids and used without further purification. The phenomena presented here were reproducible.

Structure determination combined charge flipping and simulated annealing methods. Charge flipping, as implemented in Superflip,[20] was utilized to locate the heavy (Zn) atoms. Cyanide moieties were added to the model and their positions determined by simulated annealing within TOPAS.[21] Residual electron density, not associated with the $Zn(CN)_2$ framework, was modeled using dummy atoms with large atomic displacement parameters.[22] The atomic displacement parameters for the dummy atoms were monitored to ensure no overlap with the framework electron density. Framework void volumes were evaluated within PLATON.[23] Equations-of-state were fit to the pressure-dependent lattice volumes within EOSfit.[24]

RESULTS

The high-pressure behavior of $Zn(CN)_2$ was found to differ significantly depending on the pressure-transmitting fluid. Fluid-dependent high-pressure phenomena have previously been documented but only in framework materials with porosity.[25,26] As such, fluid-dependent behavior is unexpected for the interpenetrated $Zn(CN)_2$ structure which is without guest-accessible porosity. Five distinct sequences of high-pressure phenomena were observed for the experimental conditions explored here. These are summarized in Figure 1 and Table 1. Selected data and Rietveld fits are shown in Figure 2.

Isopropanol, Ethanol, Fluorinert, Dry: $Zn(CN)_2$-I to $Zn(CN)_2$-II. Upon compression without fluid or in larger molecule fluids, similar behaviors were evident. This includes in isopropanol, FC-75, and, as reported elsewhere,[27] in dry methanol−ethanol. Framework compression was observed at pressures up to 1.50 GPa, whereupon a transition to a lower

Table 1. Selected Structural Parameters for the $Zn(CN)_2$ Phases

phase	space group	unit cell, Å	V, Å^3	Z	V/Z, Å^3	P, *GPa*
I	$Pn\bar{3}m$	a = 5.9132(7)	206.76(7)	2	103	0.00
II	*Pbca*	a = 12.2029(15)	704.94(15)	8	88	1.58
		b = 7.6698(10)				
		c = 7.5319(9)				
dia	$Fd\bar{3}m$	a = 11.29(14)	1439(3)	8	180	1.25
lon	$P6_3/mmc$	a = 8.2391(3)	780.11(11)	4	195	0.92
		c = 13.2699(17)				
pyr	$Pa\bar{3}$	a = 12.7198(3)	2058.97(8)	12	172	1.82

dx.doi.org/10.1021/ja4012707 | J. Am. Chem. Soc. 2013, 135, 7621−7628

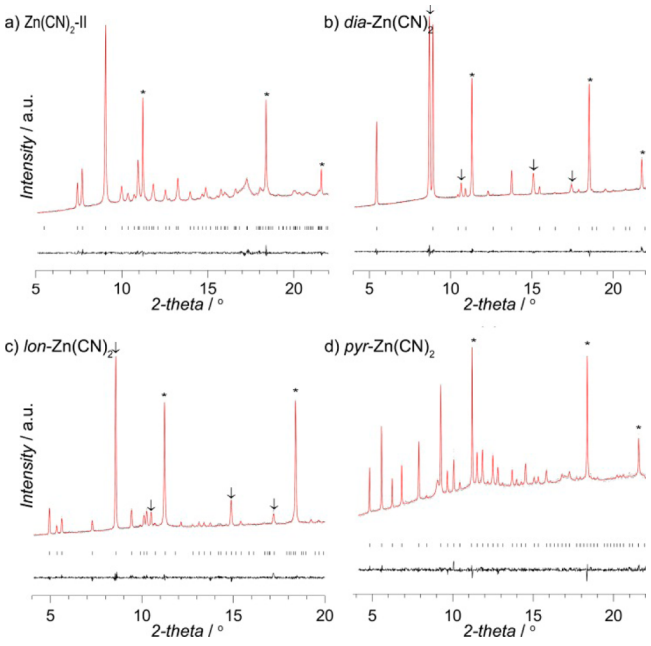

Figure 2. High-pressure powder diffraction data (dots) and the corresponding Rietveld fits (line). Peaks associated with the pressure marker (*), and residual $Zn(CN)_2$-I (↓) are indicated.

symmetry phase occurred. This phase, referred to as $Zn(CN)_2$-II, could be indexed as orthorhombic, *Pbca*, with lattice dimensions: a = 12.2029(15) Å, b = 7.6698(10) Å, c = 7.5319(9) Å, V = 704.94 (15) Å^3 at 1.58 GPa. $Zn(CN)_2$-II is related to $Zn(CN)_2$-I via a group−subgroup relationship ($a' \approx 2a$, $b' \approx a\sqrt{2}$, $c' \approx a\sqrt{2}$). The transition was accompanied by a 6.5% reduction in equivalent volume. With decompression, the transition was reversed to recover pristine cubic $Zn(CN)_2$-I.

$Zn(CN)_2$-II shares the doubly interpenetrated diamondoid structure ("*dia-c*") of $Zn(CN)_2$-I. Reduced symmetry allows for ordered distortion of the linear Zn−CN−Zn′ bridges with asymmetric displacement of the CN ligand and reorientation of the $Zn(C/N)_4$ tetrahedra (Figures 1 and 3). The asymmetric displacement of the bridging CN ligand has been suggested by multinuclear NMR studies.[28] The displacive nature of this transition is consistent with its reversibility.

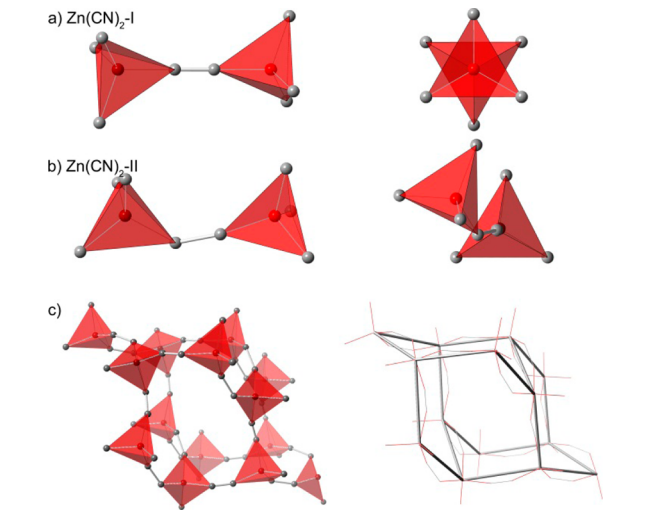

Figure 3. Representations of the connected $Zn(C/N)_4$ tetrahedra in (a) $Zn(CN)_2$-I, which has the ideal diamondoid topology, and (b) $Zn(CN)_2$-II, which has a distorted diamondoid topology. (c) The distorted $Zn(CN)_2$-II structure.

The compressibility of $Zn(CN)_2$-I and $Zn(CN)_2$-II are maximized close to the transition pressure, with softening of $Zn(CN)_2$-I and very pronounced stiffening of $Zn(CN)_2$-II upon increasing pressure (Figure 3). While cubic $Zn(CN)_2$-I compresses isotropically, highly anisotropic behavior is observed for $Zn(CN)_2$-II. The *a*-axis expands, and the *b*- and *c*-axes contract with increasing pressure. This negative linear compressibility, which occurs parallel to the *a*-axis, has been documented in a growing number of three-dimensional framework materials.[29]

A third-order Burch−Murnaghan equation-of-state fit[24] to the variable pressure lattice volumes of the $Zn(CN)_2$-I yielded the following values for the bulk modulus, and it is pressure dependence: K_0 = 34.49(22) GPa, K' = −8.48 (15), (V_0 = 202.274(21) Å^3, K″ = −4.27 GPa^{-1}). These are consistent with those reported in earlier variable pressure neutron scattering studies over a smaller pressure range.[15] The high-pressure phase, $Zn(CN)_2$-II, is initially more compressible than the parent phase (at pressures close to or just above the transition) indicating a strong pressure dependence of the bulk modulus: K_{trans} = 5.67(20) GPa, K' = 11.2(5), (V_0 = 710.0 (9) Å^3, K'' = −11 GPa^{-1}).[30]

While the separation of the interpenetrated *dia* frameworks is too small to admit guests in $Zn(CN)_2$-I or $Zn(CN)_2$-II, inefficient space filling by the frameworks is associated with an interstitial volume (Figure 5). This interstitial volume could not be evaluated directly using conventional approaches, e.g., using

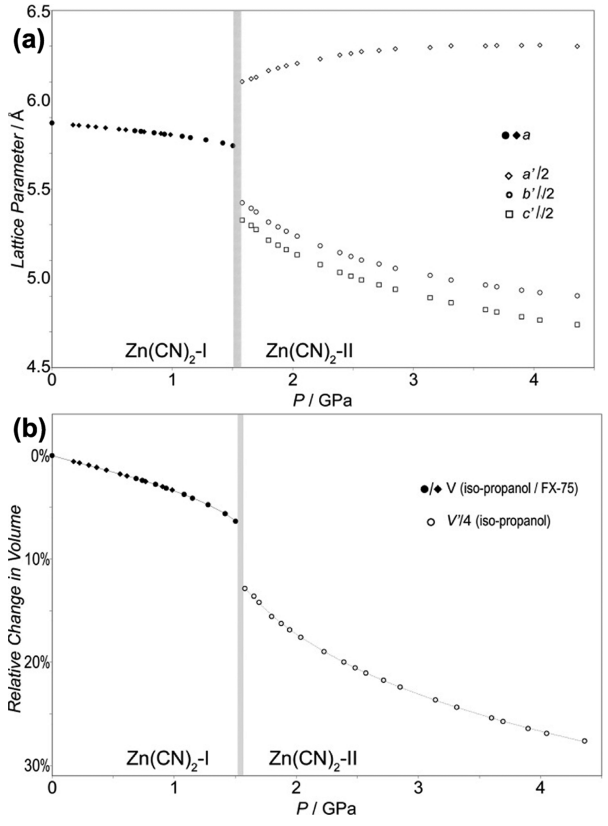

Figure 4. Pressure dependence of the lattice (a) parameters and (b) volume for $Zn(CN)_2$ in isopropanol fluid. Data from several experiments have been combined.

dx.doi.org/10.1021/ja4012707 | J. Am. Chem. Soc. 2013, 135, 7621−7628

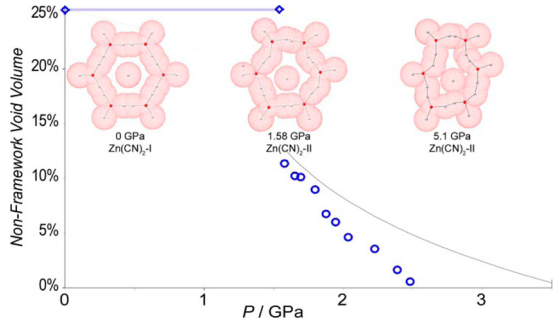

Figure 5. Estimated interstitial volume for $Zn(CN)_2$-I and $Zn(CN)_2$-II. Cross sections of the lattice at selected pressures with the van der Waals surface illustrating how the interstitial volume and framework separation varies with pressure.

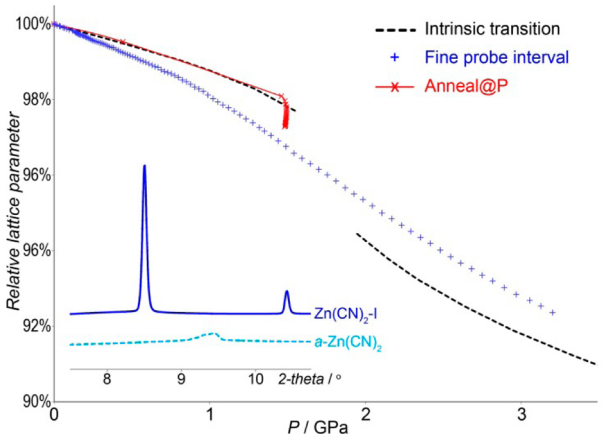

Figure 6. Impact of X-ray exposure on the framework compression in isopropanol. Selected diffraction data are inset.

the VOID routine within PLATON which considers guest-accessible voids (>1.2 Å). Instead we estimated the interstitial volume by evaluating the guest-accessible void volume for a single framework (*dia*) derived from the refined structural models and extrapolating to the interpenetrated system (*dia-c*). This approach assumes that each framework is independent of the other, with no interframework bonding interactions. For $Zn(CN)_2$-I, the interstitial volume calculated in this way is constrained to a constant value (~25–26%) due to the symmetry of the structural model. Upon transition to $Zn(CN)_2$-II, this interstitial volume is reduced to ~13%. With further increases in pressure, the interstitial volume decreases approximately linearly, becoming negligible close to 2.5 GPa. At pressures beyond 2.5 GPa, the value of the interstitial volume estimated in this way becomes negative. This unphysical value indicates a breakdown of the assumption that the interpenetrated frameworks can be considered independently and may reflect a close approach of the interpenetrated frameworks, that is, within the van der Waals radii, with new bonds formed between the frameworks. This is supported by a reduction in the interframework Zn···C/N distance at high pressures (see SI). In a related contemporary study to higher pressures,[27] the interframework bonding is clearly linked to a change in the Zn coordination; the Zn cations adopt distorted octahedral geometries.

Amorphization: *a*-$Zn(CN)_2$. Different high-pressure behavior was observed when the measurements in isopropanol were undertaken at more finely spaced pressure intervals (a factor of 5 times slower compression, over several hours), with the goal of precisely determining the transition pressure. Specifically, a significant increase in compressibility was evident, and the transition to $Zn(CN)_2$-II was not observed (Figure 6). Instead, the Bragg peaks progressively broadened during the measurement, becoming difficult to distinguish from the background beyond ~3 GPa, to form a noncrystalline (or amorphous) phase, *a*-$Zn(CN)_2$. The amorphization occurs within the hydrostatic limits of the pressure transmitting medium and is, therefore, not associated with deviatoric stress.[31] The well-defined Bragg peaks did not return upon pressure release, indicating that the amorphization was not reversible at ambient conditions.

This amorphization of $Zn(CN)_2$ was found to correlate with the X-ray exposure during the compression rather than the compression rate. Measurements using a reduced compression rate, but fewer exposures, did not show amorphization. While at ambient pressure, X-ray exposure has no discernible impact on the $Zn(CN)_2$ lattice, and at constant elevated pressure, X-ray exposure was found to affect a progressive reduction in the lattice parameter (Figure 6).

The observed loss crystallinity is not interpreted as framework decomposition or collapse. Indeed transitions to noncrystalline phases under pressure—a pressure-induced amorphization—are widely established in frameworks such as this, formed by corner-linked polyhedral units, including in zeolites and other NTE materials.[32] In these systems, the amorphization involves distortions of the framework structure and possible increases in coordination number, without decomposition.[26a,32d−f]

While pressure-induced amorphization in flexible frameworks is not without precedence,[26a,32] the coupling of this effect with X-ray exposure is unusual. We postulate that the enhanced compression observed during prolonged X-ray exposure is likely associated with X-ray excitation, whereby, at elevated pressure the X-ray excitation can also contribute to volume reduction. This may involve inducing static distortions of the Zn−CN−Zn′ linkages, such as in $Zn(CN)_2$-II, or interframework bonding interactions, as evident in $Zn(CN)_2$-II at higher pressures. The greater compressibility evident with prolonged X-ray exposure during compression of $Zn(CN)_2$-I diminishes the volume reduction associated with a transition from $Zn(CN)_2$-I to $Zn(CN)_2$-II to the point that this transition is suppressed. The higher symmetry $Zn(CN)_2$-I phase persists to higher pressures and continues to compress due to increasing dynamic distortions and localized static defects. Progressive amorphization occurs as the localized static defects, which are not ordered within the structure, start to dominate.

The influence of X-ray exposure on the lattice dimensions may contribute to variability in reports of equation-of-states fit to compression data for $Zn(CN)_2$-I. To exclude the possibility of X-ray exposure influencing the particular crystalline phase observed at high pressure, transitions observed were verified with additional measurements by minimal or no X-ray exposure below the transition pressure.

Water-Containing Fluid: *dia*-$Zn(CN)_2$. Transitions to different crystalline phases were observed upon compression in water/isopropanol fluid mixtures. Under these conditions, $Zn(CN)_2$-I transforms to a second cubic phase, referred to as *dia*-$Zn(CN)_2$, at pressures of ~1.2 GPa. This phase can be indexed in the *Fd*-3*m* space group with a = 11.29 Å at 1.25 GPa ($a' \approx 2a$). The completeness of the transition depends on the quantity of sample used. When a large amount of sample was

dx.doi.org/10.1021/ja4012707 | J. Am. Chem. Soc. 2013, 135, 7621−7628

used, to optimize the measured X-ray scattering intensities, the conversion was incomplete. Non-hydrostatic conditions limited studies beyond ~2.5 GPa. Upon release of applied pressure (to 0 GPa), the *dia*-$Zn(CN)_2$ phase was retained.

The structure of *dia*-$Zn(CN)_2$ shares the undistorted diamondoid framework of $Zn(CN)_2$-I but is without network interpenetration (Figure 7).[12] The framework density is

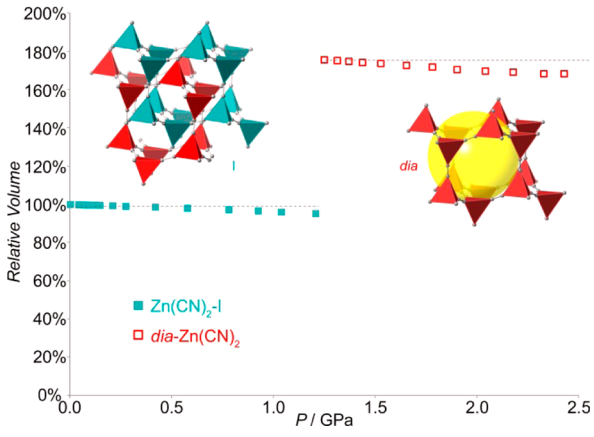

Figure 7. Relative lattice volume per $Zn(CN)_2$ formula unit upon compression in water-rich fluid. Representations of the structures, on the same scale, are inset. The maximum diameter sphere that can be contained within the framework cavities is shown in yellow.

approximately half that of $Zn(CN)_2$-I. The framework defines a diamondoid pore network, which comprises ~60% of the total crystal volume. The pore network contains interconnected cavities of ~6 Å diameter, based on a van der Waals framework surface.

The porous non-interpenetrated structure of *dia*-$Zn(CN)_2$ is known in other metal cyanides (e.g., $Cd(CN)_2 \cdot CCl_4$ clathrate and tetramethylammonium copper(I) zinc(II) cyanide), where guests occupy the pores in the as prepared material.[33,11] In *dia*-$Zn(CN)_2$, significant electron density was observed within the pores suggesting the presence of guests. For these data, the guests cannot be reliably modeled by an ordered arrangement of discrete molecules. The guests are presumed to be water, rather than larger isopropanol molecules. In this case, isopropanol was considered as an inert cofluid that extends the hydrostatic limit of the fluid mixture beyond that of pure water. The electron density in the pores corresponded to an approximate composition of $Zn(CN)_2 \cdot \sim 1\{H_2O\}$ (see SI). The pore content did not change with increasing pressure.

In the presence of water, the compression behavior below the transition mirrors that observed in isopropanol, ethanol, or fluorinert. The transition is associated with an ~80% increase in framework volume. The non-interpenetrated phase is more compressible than the double interpenetrated $Zn(CN)_2$-I. An equation-of-state fit to the variable pressure lattice volumes yielded the following parameters: K_0 = 16.6(4) GPa, K' = 4.7, V_0 = 1535.9 (25) Å^3, (K'' = −0.3 GPa^{-1}).[30] The zero pressure equivalent volume is close to double that of $Zn(CN)_2$-I.

Methanol–Ethanol–Water and Methanol: *lon*- and *pyr*-$Zn(CN)_2$. Related high-pressure behaviors were observed in MEW and pure methanol fluids, that again differed from those observed under other fluids. Upon compression in MEW, the cubic $Zn(CN)_2$-I transformed to a hexagonal $P6_3/mmc$ phase at ~1.2 GPa, referred to as *lon*-$Zn(CN)_2$, with a = 8.2169(6) Å, c = 13.1705(17) Å at 1.50 GPa. Again, the completeness of the transition depended on the quantity of sample used. With further compression, transformation to yet a third cubic phase was observed at 2.2 GPa. This phase, referred to as *pyr*-$Zn(CN)_2$, was indexed with *Pa*-3 symmetry, a = 12.72 Å ($a' \approx 2a$). In neat methanol, $Zn(CN)_2$ transforms directly to *pyr*-$Zn(CN)_2$ between 1.5 and 1.8 GPa, without evidence of *lon*-$Zn(CN)_2$. In both MEW and methanol, *pyr*-$Zn(CN)_2$ converted to *lon*-$Zn(CN)_2$ during decompression, with the *lon*-$Zn(CN)_2$ structure being retained at ambient pressure (see SI). Upon exposure to atmospheric conditions, a gradual lattice contraction is observed in *lon*-$Zn(CN)_2$, with reducing intensity of selected peaks, consistent with liberation of guest molecules from the pores without collapse of the framework structure.

The $P6_3/mmc$ phase, *lon*-$Zn(CN)_2$, consists of $Zn(C/N)_4$ tetrahedra interconnected to form a lonsdaleite framework structure (Figure 8).[12] This topology is defined by a different

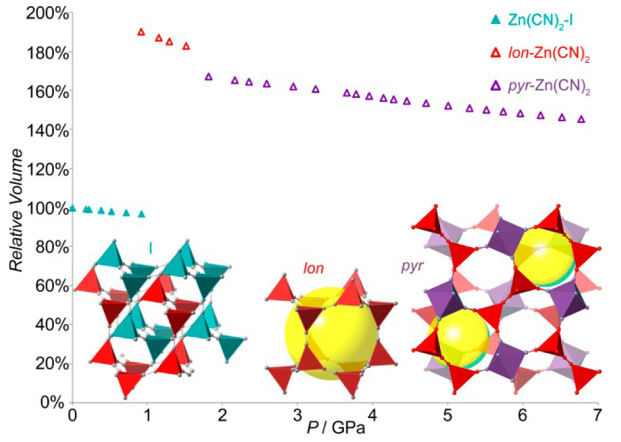

Figure 8. Relative lattice volume per $Zn(CN)_2$ formula unit upon compression in MEW fluid. Representations of the structures, on the same scale, are inset. The maximum diameter sphere that can be contained within the framework cavities is shown in yellow.

relative orientation of the linearly bridged tetrahedra than the diamondoid framework (see Figure 1). Again, the framework density is approximately half that of $Zn(CN)_2$-I. Frameworks with this structure have previously been documented for Cd cyanide clathrates.[33] The framework defines a three-dimensional pore network of linear channels (maximal dimensions of ~6 Å), aligned parallel to the c-axis and bridged in the perpendicular directions. This pore network accounts for ~60% of the total crystal volume.

In *pyr*-$Zn(CN)_2$, Zn in tetrahedral and octahedral coordination environments is connected by approximately linear cyanide bridges to form a framework with a modified pyrite topology (see Figures 1 and 8).[12] Some disordered vacancies of the CN ligand, and possible coordination of guest molecules, likely exist to maintain framework neutrality. A structural model describing the vacancy disorder and possible C/N ordering (as permitted by the framework symmetry) is beyond the resolution and sensitivity of the data. The framework defines a three-dimensional pore network with maximal cavities of ~3 Å diameter, accounting for ~50% of the total crystal volume.

In both *lon*-$Zn(CN)_2$ and *pyr*-$Zn(CN)_2$, significant electron density was observed within these pores indicating the presence of guests, however the guests could not be reliably modeled by an ordered arrangement of discrete molecules. For *lon*-$Zn(CN)_2$, the electron density in the pores corresponded to an approximate composition of $Zn(CN)_2 \cdot \sim 1/2\{CH_3OH\}$ (see

dx.doi.org/10.1021/ja4012707 | J. Am. Chem. Soc. 2013, 135, 7621−7628

SI). This electron density analysis was less reliable for *pyr*-$Zn(CN)_2$ due to the disordered nature of the framework structure. Upon exposure of *lon*-$Zn(CN)_2$ to atmosphere at ambient pressure, allowing residual alcohol fluid and guest molecules to evaporate, the pore occupancy dropped to zero without collapse of the framework structure (see SI).

The framework compression below the transition is again comparable to that observed in other fluids. The transition $Zn(CN)_2$-I to *lon*-$Zn(CN)_2$ is associated with a ~93% increase in equivalent lattice volume. The ensuing transition to *pyr*-$Zn(CN)_2$ is associated with a ~15% reduction in lattice volume. Equations-of-state fit to the data yielded the following parameters: For *lon*-$Zn(CN)_2$ K_0 = 24(4) GPa, K' = 4.4, V_0 = 808(10)Å^3; for *pyr*-$Zn(CN)_2$ K_{trans} = 24.3(5) GPa, K' = 4.7, V_{trans} = 2078(4) Å^3.[30] For *lon*-$Zn(CN)_2$, the zero pressure equivalent volume is approximately double that of the initial material, $Zn(CN)_2$-I.

DISCUSSION

The transition to $Zn(CN)_2$-II is the intrinsic high-pressure behavior of $Zn(CN)_2$, occurring without change to the composition and in the absence of pressure-transmitting media. As expected, the lattice volume reduces monotonically with increasing pressure.

While in $Zn(CN)_2$-I, the interstitial volume is not guest accessible, it represents approximately a quarter of the total crystal volume. This narrow (<1 Å), continuous void space between the interpenetrated nets is a consequence of a mismatching in the aperture defined in one net and the cross-sectional area of the interpenetrated net. In $Cd(CN)_2$, the greater M···M′ distance and, accordingly, larger interstitial volume allow small molecules to be included at low temperature.[13] Compression of $Zn(CN)_2$ involves increasing dynamic then static distortion of linear Zn−CN−Zn′ links, that reduce the Zn···Zn′ distance and the nonframework void volume. In $Zn(CN)_2$-I, the CN bridges are dynamically displaced from the Zn···Zn′ axis, evident as an increase in the atomic displacement parameters for the CN bridge normal to this axis.[15] An abrupt reduction in the void volume accompanies the transition to $Zn(CN)_2$-II, involving static distortion of the Zn−CN−Zn′ links. Compression of $Zn(CN)_2$-II is initially dominated by further distortion of the Zn−CN−Zn links which progressively eliminates voids between the interpenetrated frameworks. As pressure is increased further, compression involves progressive changes of the Zn coordination environment. This evolution in the compression mechanism contributes to the pronounced pressure-induced stiffening quantified as a large (and positive) pressure dependence of the bulk modulus (K') for $Zn(CN)_2$-II. Softening of $Zn(CN)_2$-I with increasing pressure and high compressibility of $Zn(CN)_2$-II immediately following the transition is consistent with earlier suggestions that deviation from the ideal Zn−CN−Zn′ geometry increases the flexibility of this moiety.[15]

Remarkably, transformations upon hydrostatic compression in small molecule fluid reduce the framework density and increase the crystal volume—an expansion under pressure! The 2-fold pressure-induced percentage volume expansion is 50−100 times larger than that previously observed in zeolites due to superhydration or cation migration (~100% cf. 0.8−2.5% volume expansion).[35] While the increase in volume may seem surprisingly large, the resulting new phases contain guest-filled pores, such that the overall system volume (solid sample and fluid medium) is reduced. This eliminates inefficiencies in space filling associated with the interpenetrated structure ($Zn(CN)_2$-I).

The fluid-dependent transitions occur at pressures below the intrinsic transition, where the precise transition pressure likely depends on the properties of the fluid (molecular size, density, compressibility, etc) and their temperature dependence. In fluorinert and isopropanol, the fluid molecules are presumably too large to be accommodated within the $Zn(CN)_2$ lattice at pressures below the intrinsic transition. A consequence of the fluid-driven nature of these transitions and the near 2-fold volume expansion is that the completeness of the transitions is influenced by the quantity of sample enclosed within the diamond anvil cell, that is, on the sample-to-fluid ratio and on the available (non-solid) volume within the pressure cell. Without sufficient fluid or available volume, the transitions could not proceed to completion. In these cases, the larger volume metastable phase recovered at ambient pressure was firmly wedged in the sample cavity, evident as strain broadening in the diffraction data.

Prior high-pressure studies of porous molecular frameworks have demonstrated the potential for fluid molecules to progressively fill the pores with increasing pressure.[25] The present data suggest that no significant variation in the pore composition occurs with increasing pressure (outside of the transition itself). The porous phases show similar or enhanced compressibility compared to the nonporous parent phase (as expected based on their closely related connectivities), which is consistent with this pore occupancy.

The structure-directing influence of fluids on the topology of the porous phase can be rationalized by considering the analogous $Cd(CN)_2$ clathrates.[33,34] These analogues of *dia*-$Zn(CN)_2$ and *lon*-$Zn(CN)_2$ are synthesized directly with molecules from the solvent used in synthesis included as guests.[36] Different solvents or solvent mixtures promote different framework topologies. For example, *dia*-$Cd(CN)_2$ is favored for guests with tetrahedral geometries (CCl_4, $CHCl_3$, etc), well matched to the diamondoid topology of the pores.[33] Bulky guests direct formation of *lon*-$Cd(CN)_2$, wherein larger guests can be accommodated by the linear channels.[34] Here, the tetrahedral geometry of a hydrogen-bonded water network may influence formation of *dia*-$Zn(CN)_2$, while the larger molecules in MEW or methanol favor *lon*-$Zn(CN)_2$. It is possible that other fluids may generate different porous $Zn(CN)_2$ phases including distorted diamondoid or *neb* topologies.[37,12]

The non-interpenetrated *dia*-$Zn(CN)_2$ and *lon*-$Zn(CN)_2$ can only be formed from the doubly interpenetrated parent through major bond rearrangements. The reconstructive nature of the transition means that there is an energy barrier to regenerating the initial phase and connectivity. This contributes to the metastability of these phases, which are retained when the pressure is released to 0 GPa (ambient pressure). Metastability of this type is a general characteristic of open framework systems, including MOFs or zeolites. The preliminary guest-desolvation study of *lon*-$Zn(CN)_2$, in which residual fluid and guests molecules were allowed to evaporate, suggests that it is possible to obtain a stable guest-free pore network suitable for guest sorption applications, as has been achieved for the Cd analogues.[38] Further, the thermal expansion behavior of the $Zn(CN)_2$ polymorphs could be directly compared. A significant enhancement in the NTE effect is anticipated for the non-

dx.doi.org/10.1021/ja4012707 | J. Am. Chem. Soc. 2013, 135, 7621−7628

interpenetrated systems compared to $Zn(CN)_2$-I, as has been documented in the Cd analogues.[38]

The application of hydrostatic pressure offers a distinct approach to mechanochemical syntheses of framework materials compared to established techniques, such as ball milling or grinding.[39] While milling exploits localized high pressures and temperatures to drive reactions, hydrostatic compression subjects materials to milder, homogeneous conditions, thereby allowing a different region of phase space to be explored. Additionally, the extreme fluid dependence observed for $Zn(CN)_2$ suggests that the pressure-transmitting medium may provide an additional means to manipulate the resulting phase structure. In these ways, hydrostatic pressures can generate new materials and phases not accessible through conventional synthesis or other mechanochemical approaches.

Parallels exist between the high pressure phase transitions observed for $Zn(CN)_2$ and those of other tetrahedrally connected networks. β-cristobalite (*dia*) and β-tridymite (*lon*) are known forms of SiO_2 which, as for $Zn(CN)_2$, are metastable at ambient pressure. A transition to *pyr*-SiO_2 is known, although this occurs at much higher pressures than seen here for $Zn(CN)_2$ (205 GPa cf. 1.8 GPa).[40] A high pressure form of ice with *Pbca* symmetry, related to $Zn(CN)_2$-II, has been predicted based on density functional studies.[41]

The challenge in developing a coherent description of the high pressure behavior of zinc cyanide is due to the complexity and variety of behaviors possible for this seemingly simple framework structure. In some cases, measures intended to improve sensitivity and precision (e.g., probing at finer intervals to better define transition pressures or with maximized sample loading to increase scattering signal) led to different outcomes. In light of the present results, the earlier high-pressure studies of $Zn(CN)_2$ can be reconciled.[16,17] The sequence of transitions identified in MEW ($Zn(CN)_2$-I → *lon*-$Zn(CN)_2$ → *pyr*-$Zn(CN)_2$) is apparent in an earlier study, however, the phases were not correctly indexed, and no structures were reported; the tentative (and ultimately incorrect) space group assignments were based on the assumption that the lattice density would increase at higher pressures.[16] Observations of amorphization[17] can now be ascribed to X-ray exposure at pressure.

CONCLUSION

In summary, we have shown that application of pressure to a nonporous interpenetrated framework system, in the presence of small molecule pressure-transmitting fluids, provides a novel approach to form new porous materials that may not be accessible through conventional synthetic methods. This opposes established strategies to optimize porosity that eschew both pressure/stress and framework interpenetration. We postulate that the inefficient space filling of the interpenetrated framework system is central to the pressure-induced reconstructive transition. Specifically, the transition is driven by an increase in overall atomic packing density allowed by including fluid molecules, from the pressure cell, in the pores of a metastable open framework. Not only is porosity generated under pressure but also the framework expands instead of densifying as expected under pressure. These inefficiencies in space filling are likely to be a general characteristic of interpenetrated framework systems, and consequently, it may be possible to access a broad range of new porous framework materials in this way.

The pressures required to form these new porous frameworks are low compared to those at which phase transitions are observed in traditional solid-state materials, such as metal oxides or silicates. These lower range pressures can be applied to materials on an industrial scale, not only allowing pressure to be utilized as a tool for materials synthesis but also enabling bulk sample preparation to evaluate the functional properties of the new phases. Experiments are planned to explore the host–guest chemistry and thermal expansion properties of the new $Zn(CN)_2$ polymorphs reported here. Future studies will be expanded to related systems, including $Cd(CN)_2$, $Mn(CN)_2$, $Zn_xCd_{1-x}(CN)_2$ solid-solutions,[12,42] to other anticuprite phases, to other MOFs that show interpenetration, and to a wider range of fluid media.

ASSOCIATED CONTENT

Supporting Information

Details of powder diffraction experiments, powder X-ray crystallographic information files (CIF) for $Zn(CN)_2$-II, *dia*-$Zn(CN)_2$, *lon*-$Zn(CN)_2$, *pyr*-$Zn(CN)_2$. This material is available free of charge *via* the Internet at http://pubs.acs.org.

AUTHOR INFORMATION

Corresponding Author

chapmank@aps.anl.gov

Author Contributions

[§]These authors contributed equally

Notes

The authors declare no competing financial interest.

ACKNOWLEDGMENTS

Work done at Argonne and use of the Advanced Photon Source, an Office of Science User Facility operated for the U.S. Department of Energy Office of Science by Argonne National Laboratory, were supported by the U.S. Department of Energy under contract no. DE-AC02-06CH11357.

REFERENCES

(1) *Handbook of Zeolite Science and Technology*; Auerbach, S. M., Carrado, K. A., Dutta, P. K., Ed.; Marcel Dekker, Inc.: New York, 2003.

(2) (a) Li, J. R.; Kuppler, R. J.; Zhou, H. C. *Chem. Soc. Rev.* **2009**, *38*, 1477. (b) Kitagawa, S.; Kitaura, R.; Noro, S. *Angew. Chem., Int. Ed.* **2004**, *43*, 2334.

(3) (a) Chapman, K. W.; Chupas, P. J.; Nenoff, T. M. *J. Am. Chem. Soc.* **2010**, *132*, 8897. (b) Sava, D. F.; Rodriguez, M. A.; Chapman, K. W.; Chupas, P. J.; Greathouse, J. A.; Crozier, P. S.; Nenoff, T. M. *J. Am. Chem. Soc.* **2011**, *133*, 12398. (c) Chapman, K. W.; Sava, D. F.; Halder, G. J.; Chupas, P. J.; Nenoff, T. M. *J. Am. Chem. Soc.* **2011**, *133*, 18583.

(4) Eddaoudi, M.; Kim, J.; Rosi, N.; Vodak, D.; Wachter, J.; O'Keefe, M.; Yaghi, O. M. *Science* **2002**, *295*, 469.

(5) Moulton, B.; Zaworotko, M. J. *Chem. Rev.* **2001**, *101*, 1629.

(6) Batten, S. R.; Robson, R. *Angew. Chem., Int. Ed.* **1998**, *37*, 1460.

(7) Bennett, T. D.; Cao, S.; Tan, J. C.; Keen, D. A.; Bithell, E. G.; Beldon, P. J.; Friscic, T.; Cheetham, A. K. *J. Am. Chem. Soc.* **2011**, *133*, 14546.

(8) Farha, O. K.; Hupp, J. T. *Acc. Chem. Res.* **2010**, *43*, 1166.

(9) Nelson, A. P.; Farha, O. K.; Mulfort, K. L.; Hupp, J. T. *J. Am. Chem. Soc.* **2009**, *131*, 458.

(10) Williams, D. J.; Partin, D. E.; Lincoln, F. J.; Kouvetakis, J.; O'Keeffe, M. *J. Solid State Chem.* **1997**, *134*, 164.

(11) Hoskins, B. F.; Robson, R. *J. Am. Chem. Soc.* **1990**, *112*, 1546.

(12) O'Keeffe, M.; Peskov, M. A.; Ramsden, S. J.; Yaghi, O. M. *Acc. Chem. Res.* **2008**, *41*, 1782–1789.

(13) Goodwin, A. L.; Kepert, C. J. *Phys. Rev. B* **2005**, *71*, 140301.
(14) Chapman, K. W.; Chupas, P. J.; Kepert, C. J. *J. Am. Chem. Soc.* **2005**, *127*, 15630.
(15) Chapman, K. W.; Chupas, P. J. *J. Am. Chem. Soc.* **2007**, *129*, 10090.
(16) Poswal, H. K.; Tyagi, A. K.; Lausi, A.; Deb, S. K.; Sharma, S. M. *J. Solid State Chem.* **2009**, *182*, 136.
(17) Shekar, N. V. C.; Ravindran, T. R.; Sahu, P. C.; Arora, A. K. *Indian J. Phys.* **2009**, *83*, 1289.
(18) (a) Hammersley, A. P. ESRF Internal Report 1997, ESRF97HA02T. (b) Hammersley A. P., Svensson, S. O., Hanfland, M., Fitch, A. N., Häusermann D. *High Pressure Res.*, **1996**, *14*, 235.
(19) (a) Hazen, R. M.; Finger, L. W. *J. Phys. Chem. Solids* **1981**, *42*, 143. (b) Decker, D. L. *J. Appl. Phys.* **1971**, *42*, 3239−3244.
(20) Coelho, A. A.; Evans, J. S. O.; Evans, I. R.; Kern, A.; Parsons, S. *Powder Diffr.* **2011**, *26*, S22.
(21) Palatinus, L.; Chapuis, G. *J. Appl. Crystallogr.* **2007**, *40*, 786.
(22) A related approach is regularly used in refining structure models based on single crystal diffraction data using the SQUEEZE routine within PLATON.[23] This approach does not degrade the reliability of the framework structure.
(23) Spek, A. L. *Acta Crystallogr.* **2009**, *D65*, 148−155.
(24) Angel R. J. Equations of state. In *High-pressure and high-temperature crystal chemistry (Reviews in Mineralogy and Geochemistry)*; Hazen, R. M., Downs, R. T.; Eds., 2000; Vol. *41*, pp 35−60.
(25) (a) Chapman, K. W.; Halder, G. J.; Chupas, P. J. *J. Am. Chem. Soc.* **2008**, *130*, 10524. (b) Graham, A. J.; Tan, J. C.; Allan, D. R.; Moggach, S. A. *Chem. Commun.* **2012**, *48*, 1535.
(26) (a) Chapman, K. W.; Halder, G. J.; Chupas, P. J. *J. Am. Chem. Soc.* **2009**, *131*, 17546. (b) Moggach, S. A.; Bennett, T. D.; Cheetham, A. K. *Angew. Chem., Int. Ed.* **2009**, *48*, 7087.
(27) Collings, I. E.; Cairns, A. B.; Thompson, A. L.; Parker, J. E.; Tang, C. C.; Tucker, M. G.; Catafesta, J.; Levelut, C.; Haines, J.; Dmitriev, V.; Pattison, P.; Goodwin, A. L.; **2013**, DOI: 10.1021/ja401268g.
(28) Werner-Zwanziger, U.; Chapman, K. W.; Zwanziger, J. W. *Z. Phys. Chem.* **2012**, *226*, 1205.
(29) (a) Goodwin, A. L.; Keen, D. A.; Tucker, M. G. *Proc. Nat. Acad. Sci. U.S.A.* **2008**, *105*, 18708. (b) Cairns, A. B.; Thompson, A. L.; Tucker, M. G.; Haines, J.; Goodwin, A. L. *J. Am. Chem. Soc.* **2012**, *134*, 4454. (c) Li, W.; Probert, M. R.; Kosa, M.; Bennett, T. D.; Thirumurugan, A.; Burwood, R. P.; Parinello, M.; Howard, J. A. K.; Cheetham, A. K. *J. Am. Chem. Soc.* **2012**, *134*, 11940.
(30) The fitting of equations-of-state was complicated by the absence of low pressure compression data for these phases. In this case, the pressure dependence of the bulk modulus was estimated based on a data offset to lower pressures ($P_{trans} > P_0$), and its value fixed when fitting the equation-of-state. This provided values of V_0 that were more consistent with expectation (based on equivalent volume of pristine material). For phases not recoverable to ambient pressure as metastable phases, the bulk modulus at the transition pressure is reported.
(31) Angel, R. J.; Bujak, M.; Zhao, J.; Gatta, G. D.; Jacobsen, S. D. *J. Appl. Crystallogr.* **2007**, *40*, 26.
(32) (a) Hemley, R. J.; Jephcoat, A. P.; Mao, H. K.; Ming, L. C.; Manghnani, M. H. *Nature* **1988**, *334*, 52. (b) Perottoni, C. A.; da Jornada, J. A. H. *Science* **1998**, *280*, 886. (c) Bennett, T. D.; Simoncic, P.; Moggach, S. A.; Gozzo, F.; Macchi, P.; Keen, D. A.; Tan, J. C.; Cheetham, A. K. *Chem. Commun.* **2011**, *47*, 7983. (d) Readman, J. E.; Forster, P. M.; Chapman, K. W.; Chupas, P. J.; Parise, J. B.; Hriljac, J. A. *Chem. Commun.* **2009**, 3383. (e) Keen, D. A.; Goodwin, A. L.; Tucker, M. G.; Dove, M. T.; Evans, J. S. O.; Crichton, W. A.; Brunelli, M. *Phys. Rev. Lett.* **2007**, *98*, 225501. (f) Wilkinson, A. P.; Greve, B. K.; Ruschman, C. J.; Chapman, K. W.; Chupas, P. J. *J. Appl. Phys.* **2012**, 112.
(33) Iwamoto, T. J. *Inclusion Phenom. Mol. Recognit. Chem.* **1996**, *24*, 61.
(34) Kitazawa, T.; Kikuyama, T.; Takeda, M.; Iwamoto, T. *J. Chem. Soc., Dalton Trans.* **1995**, *24*, 3715.
(35) Lee, Y.; Vogt, T.; Hriljac, J. A.; Parise, J. B.; Artioli, G. *J. Am. Chem. Soc.* **2002**, *124*, 5466.
(36) Direct synthesis of *dia*-$Zn(CN)_2$ and *lon*-$Zn(CN)_2$, in the same way as the $Cd(CN)_2$ clathrates, has not been achieved. This may be due to the extreme insolubility of $Zn(CN)_2$ ($K_{sp}(25\ ^\circ C) = 3 \times 10^{-16}$); rapid crystallization of $Zn(CN)_2$ does not facilitate guest-directed self-assembly.
(37) Kitazawa, T. *Chem. Commun.* **1999**, *35*, 891.
(38) Phillips, A. E.; Goodwin, A. L.; Halder, G. J.; Southon, P. D.; Kepert, C. J. *Angew. Chem., Int. Ed.* **2008**, *47*, 1396.
(39) (a) Friscic, T. *Chem. Soc. Rev.* **2012**, *41*, 3493. (b) Bennett, T. D.; Cao, S.; Tan, J. C.; Keen, D. A.; Bithell, E. G.; Beldon, P. J.; Friscic, T.; Cheetham, A. K. *J. Am. Chem. Soc.* **2011**, *133*, 14546.
(40) Prakapenka, V. P.; Shen, G.; Dubrovinsky, L. S.; Rivers, M. L.; Sutton, S. R. *J. Phys. Chem. Solids* **2004**, *65*, 1537.
(41) Militzer, B.; Wilson, H. F. *Phys. Rev. Lett.* **2010**, *105*, 195701.
(42) (a) Kareis, C. M.; Lapidus, S. H.; Stephens, P. W.; Miller, J. S. *Inorg. Chem.* **2012**, *51*, 3046. (b) Manson, J. L.; Buschmann, W. E.; Miller, J. S. *Angew. Chem., Int. Ed.* **1998**, *37*, 783.